ELSEVIER

www.elsevier.nl/locate/carres

Carbohydrate Research 321 (1999) 75–87

CARBOHYDRATE RESEARCH

Ganglioside expression in tissues of mice lacking the tumor necrosis factor receptor 1

Anita Markotić [a], Regine Lümen [b], Ana Marušić [c], Stipan Jonjić [d], Johannes Müthing [b,*]

[a] *Department of Biochemistry, Split University School of Medicine, 21000 Split, Croatia*
[b] *Universität Bielefeld, Technische Fakultät, Arbeitsgruppe Zellkulturtechnik, Postfach 100131, D-33501 Bielefeld, Germany*
[c] *Institute for Brain Research and Basic Medical Sciences, Zagreb University School of Medicine, 10000 Zagreb, Croatia*
[d] *Department of Histology, Rijeka University School of Medicine, 51000 Rijeka, Croatia*

Received 19 April 1999; accepted 25 June 1999

Abstract

This study presents a comparative analysis of gangliosides from lymphoid (spleen and thymus) and other tissues (brain, liver, lung, muscle) of C57BL/6 mice homozygous (−/−) and heterozygous (+/−) for the tumor necrosis factor receptor 1 (TNFRp55). Quantitative and qualitative differences in the expression of the lipid-bound *N*-acetylneuraminic (Neu5Ac) and *N*-glycolylneuraminic acid (Neu5Gc) and of various ganglioside biosynthesis pathways were detected between the tissues of the TNFRp55 −/− and the control TNFRp55 +/− mice. Sialic acid profiles showed a strong decrease in the absolute amount of sialic acids (Neu5Ac + Neu5Gc) in the lungs and thymus of homozygous (1.41 and 0.3 ng/mg wet weight, respectively) compared with control heterozygous animals (7.18 and 2.05 ng/mg wet weight, respectively). Considerable differences of Neu5Ac/Neu5Gc ratios in the lungs, muscle, spleen, and thymus were also detected. The gangliosides G_{M3}(Neu5Ac) and G_{M3}(Neu5Gc) were the dominant gangliosides in the lungs of the control animals, whereas the knockout mice almost completely lacked these structures in this organ. Reduced expression of G_{M1b}-type gangliosides (G_{M1b} and GalNAc-G_{M1b}) was also found in the lungs, spleen, and thymus of the TNFRp55 knockout mice. On the other hand, neolacto-series gangliosides were more abundant in the lungs, brain, and muscle of the knockout mice, whereas their expression in the liver, spleen, and thymus was similar in both groups of animals. This study provides in vivo evidence that TNF signaling via the TNFRp55 is involved in the acquisition of a distinct ganglioside assembly in different mouse organs. TNFRp55 signaling seems

* Corresponding author. Tel.: +49-521-106-6320; fax: +49-521-106-6328.
E-mail address: jm@zellkult.techfak.uni-bielefeld.de (J. Müthing)

Abbreviations: DMB, 1,2-diamino-4,5-methylenedioxybenzene; GSL(s), glycosphingolipid(s); TNF, tumor necrosis factor; TNFRp55, TNF receptor p55. The designation of the glycosphingolipids follows the IUPAC–IUB recommendations [71] and the nomenclature of Svennerholm [72]. Lactosylceramide or LacCer, Galβ1-4Glcβ1-1Cer; gangliotriaosylceramide or $GgOse_3Cer$, GalNAcβ1-4Galβ1-4Glcβ1-1Cer; gangliotetraosylceramide or $GgOse_4Cer$, Galβ1-3GalNAcβ1-4Galβ1-4Glcβ1-1Cer; lacto-*N*-neotetraosylceramide or $nLcOse_4Cer$ or nLc4, Galβ1-4GlcNAcβ1-3Galβ1-4Glcβ1-1Cer; lacto-*N*-norhexaosylceramide or $nLcOse_6Cer$ or nLc6, Galβ1-4GlcNAcβ1-3Galβ1-4GlcNAcβ1-3Galβ1-4Glcβ1-1Cer; G_{M3}, II^3Neu5Ac-LacCer; G_{M2}, II^3Neu5Ac-$GgOse_3Cer$; G_{M1} or G_{M1a}, II^3Neu5Ac-$GgOse_4Cer$; G_{M1b}, IV^3Neu5Ac-$GgOse_4Cer$; GalNAc-G_{M1b}, IV^3Neu5Ac-$GgOse_5Cer$; G_{D3}, $II^3(Neu5Ac)_2$-LacCer; $G_{D1\alpha}$, IV^3Neu5Ac,III^6Neu5Ac-$GgOse_4Cer$; G_{D1a}, IV^3Neu5Ac, II^3Neu5Ac-$GgOse_4Cer$; G_{D1b},$II^3(Neu5Ac)_2$-$GgOse_4Cer$; G_{T1b}, IV^3Neu5Ac,$II^3(Neu5Ac)_2$-$GgOse_4Cer$. Only Neu5Ac-substituted gangliosides are presented in this list of abbreviations.

PII: S0008-6215(99)00171-8

to be especially important for the activation of the G_{M1b}-type ganglioside biosynthetic pathway that is a unique characteristic of the mouse lymphoid tissues.

Keywords: Gangliosides; Antibodies; Thin-layer chromatography (TLC) immunostaining; Gene knockout mice; TNFRp55

1. Introduction

Tumor necrosis factor-α (TNFα) binds to two different receptors, tumor necrosis factor receptor 1 (TNFRp55) and TNFRp75 (reviewed by Armitage [1]). Targeted disruption of the gene for TNFRp55 [2,3] revealed a critical function of this receptor in the morphogenesis of lymphoid organs and generation of the immune response to antigens. TNFRp55 is important for the differentiation of Peyer's patches, differentiation of follicular dendritic cells in the spleen, development of germinal centers, and T-cell-dependent antibody response [4,5]. Targeted disruption of TNFRp75 revealed that this receptor is not important for the differentiation and morphology of lymphoid organs, but may play a role in the necrotic effects of TNF [6] or in suppressing TNF-mediated inflammatory responses [7]. TNFRp55 triggers several second messenger systems, including phospholipase A2, protein kinase C, phosphatidylcholine-specific phospholipase C, and acid sphingomyelinase [8,9]. Activation of the acid sphingomyelinase generates ceramide, which can then act on a number of direct targets [10], such as protein kinase C isoform ξ, which links the TNF receptor to nuclear factor κB activation [11].

The sphingomyelin pathway links TNFRp55 to glycosphingolipids (GSLs), a large family of macromolecules built upon ceramide [12]. GSLs are ubiquitous, highly conserved membrane components with an important biological role in cell surface recognition [13,14] and modulation of function of a variety of membrane associated proteins (reviewed by Hakomori and Igarashi [15]). GSLs are assembled as 'rafts' [16] or 'glycosignaling domains' [17] in the outer leaflet of the plasma membrane, and these clustered GSLs but not nonclustered GSLs are suggested to exert their biological activities. Gangliosides are characterized by the presence of one or more sialic acid units in the oligosaccharide chain. The parent compounds are Neu5Ac and Neu5Gc, which are known to play crucial roles in various biological functions [18,19]. There is a wealth of data on the role of gangliosides in the regulation of the immune response. Such effects are, e.g., inhibition of lymphoproliferation [20] and modulation of CD4 from helper T lymphocytes [21,22], suppression of cytotoxic activity of natural killer cells [23], and inhibition of monocyte accessory function [24]. Gangliosides inhibit TNFα synthesis in monocytes [25], and can protect from TNFα-induced apoptosis [26]. Development of tumor cell resistance to TNF cytolysis is coupled to a two-fold decrease in ganglioside expression [27]. On the other hand, TNF can stimulate ganglioside expression in tumor cells in vitro [28].

As a first step in elucidating the interaction between the TNFα and GSL functions, we analyzed the lipid-bound sialic acid profiles and ganglioside pattern of different organs from mice deficient in the p55 TNF receptor in comparison with control mice heterozygous for the gene knockout. Sialic acids were quantified as their 1,2-diamino-4,5-methylenedioxybenzene (DMB) derivatives by high-performance liquid chromatography (HPLC) and the thin-layer chromatography (TLC) immunostaining technique was used to determine the differences between various ganglioside biosynthesis pathways in six tissues [29]. These highly specific and sensitive methods revealed differences in the expression of Neu5Ac and Neu5Gc and different patterns of G_{M3}(Neu5Ac) and G_{M3}(Neu5Gc), G_{M1b}-type (G_{M1b}, GalNAc-G_{M1b} and $G_{D1\alpha}$), and neolacto-series gangliosides in the tissues of the control mice and mice homozygous for the TNFRp55 gene knockout.

2. Results

This study presents a comparative investigation of gangliosides from lymphoid (spleen and thymus) and other tissues (lung, brain,

muscle, liver) of mice lacking the TNFRp55 gene. Gangliosides from C57BL/6 mice homozygous (−/−) and heterozygous (+/−; control mice) for the TNFRp55 receptor gene knockout were isolated from different organs and tissues from 10 male animals (Table 1). To analyze the qualitative and quantitative differences between Neu5Ac and Neu5Gc substitution, lipid-bound sialic acids were quantified as their DMB derivatives. Resorcinol and TLC immunostaining were performed for structural characterization. A panel of specific antibodies was employed for the immunochemical analysis of G_{M3}, G_{M1b}-type, neolacto-series, and G_{M1}-type gangliosides in the brain, liver, lungs, muscle, spleen, and thymus.

Ganglioside-derived sialic acids from different tissues of control and TNFRp55 knockout mice.—Sialic acid profiles showed considerable differences in the absolute amounts of lipid-bound sialic acids within each group of animals, depending on the tissue of origin. Comparing the sialic acid concentrations from various tissues of TNFRp55−/− or control TNFRp55+/− animals, quantitative and qualitative differences in sialic acid concentrations and Neu5Ac/Neu5Gc ratios were also observed between the same tissues of homo- and heterozygous mice (Table 2). HPLC runs of DMB derivatives of sialic acids released from lung and thymus gangliosides are shown as an example in Fig. 1. The most prominent difference in sialic acid concentrations was a strong decrease in the absolute amount of sialic acids (Neu5Ac + Neu5Gc) in the lungs and thymus of homozygous animals (1.41 and 0.3 ng/mg wet weight, respectively) compared with heterozygous animals (7.18 and 2.05 ng/mg wet weight, respectively). Furthermore, relevant changes in Neu5Ac/Neu5Gc ratios were found in lungs, muscle, spleen, and thymus (Fig. 2). The decrease in the total sialic acid concentration in the lungs and thymus of homozygous animals (Fig. 2, upper panel, Ac and Af, respectively) compared with heterozygous animals (Fig. 2, upper panel, Bc and Bf, respectively) correlated with a relative decrease of Neu5Gc versus Neu5Ac in homozygous (Fig. 2, lower panel, Ac and Af, respectively) compared with heterozygous mice (Fig. 2, lower panel, Bc and Bf, respectively; Table 2). On the other hand, an increase in ganglioside-derived Neu5Ac was observed in the brain of homozygous (Fig. 2, upper panel, Aa) compared with heterozygous animals (Fig. 2, upper panel, Ba). As a first step to attributing these differences to changes in the ganglioside expression, we performed resorcinol TLC stains.

Resorcinol staining of gangliosides from different tissues of control and TNFRp55 knockout mice.—Resorcinol-stained thin-layer chromatograms of gangliosides from different tissues of TNFRp55−/− and control TNFRp55+/− mice are shown in Fig. 3(A) and (B), respectively. Due to the different concentrations in respective organs, ganglioside amounts corresponding to 10 mg (brain; Fig. 3, lanes a), 40 mg (liver, spleen, and thymus; Fig. 3, lanes b, e, and f, respectively) and 60 mg wet weight (lung and muscle; Fig. 3, lanes c and d, respectively) were applied. Purified G_{M3}(Neu5Gc) substituted with C_{24}- and C_{16}-fatty acid (upper and lower band, respectively; Fig. 3, lanes g); ganglioside preparations from the human brain (Fig. 3, lanes h) and granulocytes (Fig. 3, lanes i) were used as references. Neolacto-series monosialogangliosides from human granulocytes chromatograph as double bands on HPTLC plates according to their ceramide C_{24}- and C_{16}-fatty acids (upper and lower bands, respectively [30]). The most obvious difference in the ganglioside expression between the control and knockout mice was a dominant G_{M3} triple

Table 1
Total wet weights of tissues obtained from mice homozygous (−/−) or heterozygous (+/−) for the TNFRp55 gene knockout [a]

Strain	Brain	Liver	Lungs	Muscle	Spleen	Thymus
TNFRp55−/−	4.203	13.768	1.463	1.378	0.671	0.554
TNFRp55+/−	4.198	14.472	1.483	1.541	0.789	0.644

[a] Wet weights of tissues obtained from 10 male mice are given in grams.

Table 2
Lipid-bound sialic acid concentrations in tissues from mice homozygous (−/−) or heterozygous (+/−) for the TNFRp55 gene knockout

Sign [a]	Tissue	Neu5Ac [b]		S.D. [c] (%)	Neu5Gc [b]		S.D. [c] (%)	Total [d] (ng/mg)	S.D. [c] (%)
		(ng/mg)	(%)		(ng/mg)	%			
Aa	Brain (−/−)	277.73	100.0	8.6	0.00	0.0		277.73	8.6
Ba	Brain (+/−)	188.19	100.0	2.6	0.00	0.0		188.19	2.6
Ab	Liver (−/−)	0.71	8.2	1.6	7.86	91.8	5.4	8.57	5.1
Bb	Liver (+/−)	0.29	3.0	10.8	9.22	97.0	4.6	9.51	4.8
Ac	Lung (−/−)	1.12	79.3	0.3	0.29	20.7	3.2	1.41	0.9
Bc	Lung (+/−)	4.12	57.4	5.4	3.06	42.6	4.4	7.18	4.9
Ad	Muscle (−/−)	0.34	44.2	19.8	0.43	55.8	5.5	0.77	11.8
Bd	Muscle (+/−)	0.37	78.0	4.6	0.10	22.0	9.2	0.47	5.6
Ae	Spleen (−/−)	2.61	69.4	7.2	1.15	30.6	6.8	3.76	7.1
Be	Spleen (+/−)	3.05	53.4	2.5	2.66	46.6	0.2	5.71	1.4
Af	Thymus (−/−)	0.24	79.2	19.3	0.06	20.8	2.8	0.30	15.9
Bf	Thymus (+/−)	1.15	56.2	7.2	0.90	43.8	3.3	2.05	5.5

[a] The abbreviations are the same as in Figs. 1–3; A, TNFRp55−/−; B, TNFRp55+/−; a, brain; b, liver; c, lung; d, muscle; e, spleen; f, thymus.
[b] ng sialic acid per mg wet weight; percentages are defined as the values against the total amount of lipid-bound sialic acids.
[c] Standard deviations (S.D.) as percentage of four measurements of each sialic acid.
[d] Total lipid-bound sialic acids (Neu5Ac+Neu5Gc), given as ng per mg wet weight.

band in the lungs of TNFRp55+/− (Fig. 3(B), lane c) compared with trace G_{M3}-quantities in TNFRp55−/− mice (Fig. 3(A), lane c). The separation of individual murine gangliosides on HPTLC plates as triple bands, such as observed here with G_{M3}, is a common feature and is due to the variation in the ceramide portion (long- and short-chain fatty acids) and oligosaccharide moiety (Neu5Ac and Neu5Gc). This results in two pairs of gangliosides, each homogeneous in their oligosaccharide but heterogeneous in their respective ceramides. These gangliosides run as a triple band: the middle band is composed of G_{M3}(Neu5Ac) with a C_{16}- and G_{M3}(Neu5Gc) with a C_{24}-fatty acid, the upper band represents G_{M3}(Neu5Ac) with a C_{24}-fatty acid and the lower band is G_{M3}(Neu5Gc) with a C_{16}-fatty acid [31,32]. Because G_{M3} was the major ganglioside in lungs of control TNFRp55+/− mice (Fig. 3(B), lane c), the strong decrease in Neu5Gc-substitution in TNFRp55−/− mice could be due to a reduced G_{M3}(Neu5Gc) expression in homozygous animals. This was verified by TLC immunostaining with specific anti-G_{M3}(Neu5Ac) and anti-G_{M3}(Neu5Gc) antibodies and is outlined in the next section. No other conclusion concerning the structural differences between the two groups of mice could be drawn from the resorcinol-stained TLCs in Fig. 3, partly because of the occurrence of resorcinol-negative bands that covered minor gangliosides (Fig. 3, lanes f). In the next step, we used a panel of GSL-specific antibodies and G_{M1}-specific choleragenoid as detection tools [33] to study the expression of G_{M3} and G_{M1b}-type (G_{M1b}, $G_{D1\alpha}$, GalNAc-G_{M1b}) gangliosides, neolacto-series gangliosides (IV^3nLc4, IV^6nLc4, and VI^3nLc6), and G_{M1a}-type gangliosides (G_{M1}, G_{D1a}, G_{D1b}, and G_{T1b})

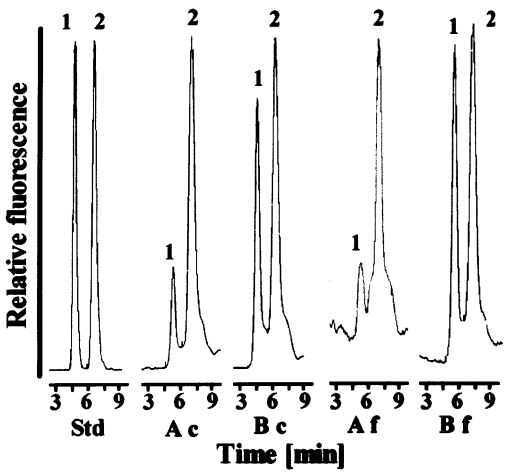

Fig. 1. HPLC elution profiles of fluorescent DMB derivatives of Neu5Gc (1) and Neu5Ac (2) released from lungs (c) and thymus (f) gangliosides of TNFRp55−/− (A) and control TNFRp55+/− mice (B). Sialic acids corresponding to 25 mg wet weight of respective organs were chromatographed. Std, Neu5Gc and Neu5Ac standards (20 ng, each). Abbreviations are the same as in Table 2.

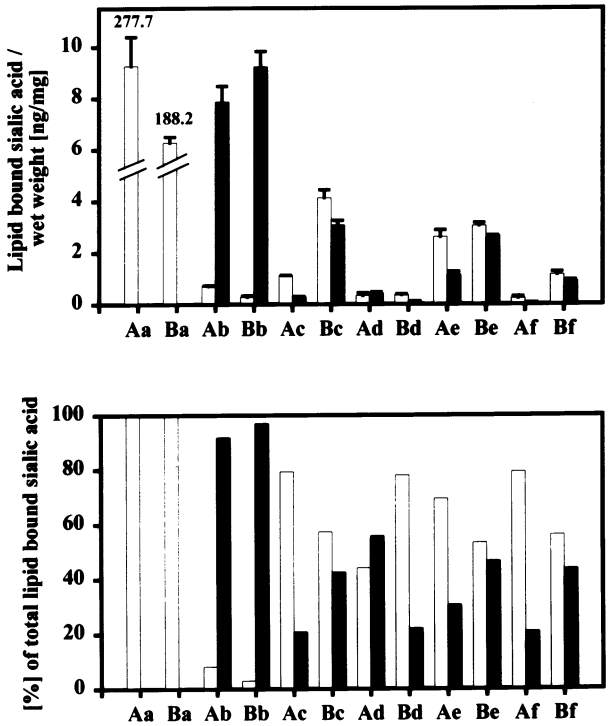

Fig. 2. Ganglioside-derived sialic acid concentrations in tissues of TNFRp55 − / − (A) and control TNFRp55 + / − mice (B). (a) Brain; (b) liver; (c) lungs; (d) muscle; (e) spleen; (f) thymus. Abbreviations are the same as in Table 2. □, Neu5Ac; ■, Neu5Gc.

in various tissues of TNFRp55 − / − and TNFRp55 + / − mice.

TLC immunostaining of G_{M3}(Neu5Ac) and G_{M3}(Neu5Gc) in lungs of control and TNFRp55 knockout mice.—TLC overlay analysis of the G_{M3} composition in the lungs of TNFRp55 + / − animals revealed the dominance of C_{24}-fatty acid-substituted G_{M3}(Neu5Ac) and G_{M3}(Neu5Gc) in the upper and middle band, respectively, whereas only small amounts of G_{M3}(Neu5Ac) and G_{M3}(Neu5Gc) with C_{16}-fatty acid were detectable in the middle and lower band, respectively. An anti-G_{M3}(Neu5Gc) TLC overlay assay of the ganglioside fraction from TNFRp55 − / − and TNFRp55 + / − animals is shown in Fig. 4(B) (lanes c and d, respectively; compare with resorcinol-stained TLC in Fig. 4(A)) together with the reference stain of G_{M3}(Neu5Gc) from a mouse hybridoma (Fig. 4(B), lane e). Brain gangliosides from both mouse strains (Fig. 4(B), lanes a and b) and human granulocyte gangliosides (Fig. 4(B), lane f) did not stain with this antibody, indicating high specificity of the anti-G_{M3}(Neu5Gc) antibody, which does not react with any ganglio- and neolactoseries gangliosides [32]. A quantitative comparison of G_{M3}(Neu5Ac) and G_{M3}(Neu5Gc) expression by TLC immunostaining with respective antisera is not possible due to different binding parameters of antibodies. Because G_{M3} makes up about 95% of the resorcinol stain (Fig. 4(A), lane d) of the lungs of TNFRp55 + / − mice, the G_{M3}(Neu5Ac)/G_{M3}(Neu5Gc) ratio should be almost identical to the values for total lipid-bound sialic acids (see Table 2). These data indicate that the lungs of control TNFRp55 + / − mice have a high expression of terminally sialylated lactosylceramide substituted with about 57% Neu5Ac and 43% Neu5Gc, whereas the lungs of TNFRp55 − / − mice almost lack this ganglioside. Therefore, the difference in the total sialic acid of 5.77 ng/mg wet weight (see Table 2 and Fig. 4(A), lanes c and d) is almost completely due to the lactosylceramide-bound sialic acids.

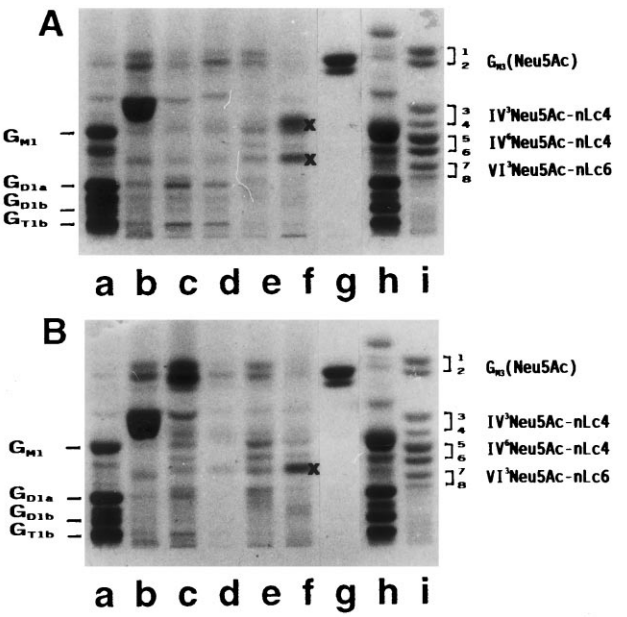

Fig. 3. Resorcinol staining of gangliosides from various tissues of TNFRp55 − / − (A) and control TNFRp55 + / − mice (B). Ganglioside amounts corresponding to 10 mg (brain, lanes a), 40 mg (liver, lanes b), 60 mg (lungs and muscle, lanes c and d, respectively) and 40 mg wet weight (spleen and thymus, lanes e and f, respectively) were chromatographed together with 3 μg G_{M3}(Neu5Gc) (lanes g), 20 μg human brain (lanes h) and 10 μg human granulocyte reference gangliosides (lanes i). Crosses indicate resorcinol negative bands. Abbreviations are the same as in Table 2.

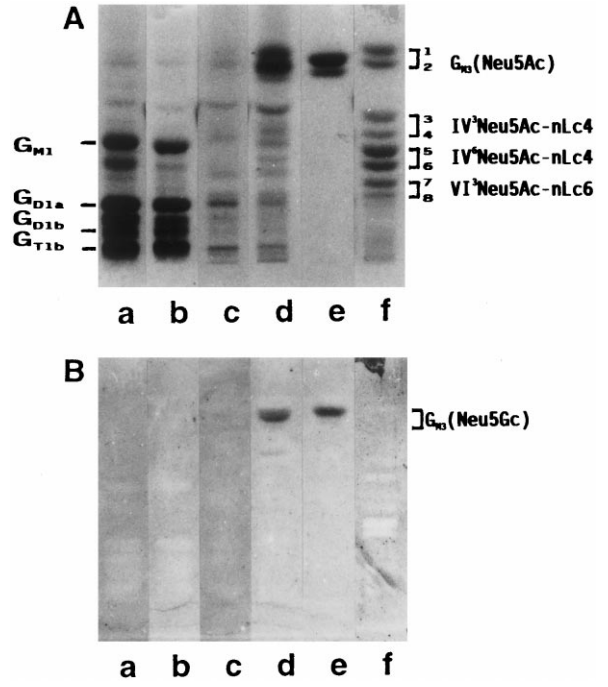

Fig. 4. Resorcinol stain (A) and anti-G_{M3}(Neu5Gc) TLC immunostain (B) of ganglioside fractions from the brain and lungs of TNFRp55 − / − and control TNFRp55 + / − mice. Panel A shows chromatograms of ganglioside amounts corresponding to 10 mg brain (TNFRp55 − / −, lane a, and TNFRp55 + / −, lane b) and 60 mg lung wet weight (TNFRp55 − / −, lane c, and TNFRp55 + / −, lane d), whereas for TLC immunostaining (panel B) one third of ganglioside quantities were applied in the same order. In both panels 3 μg of G_{M3}(Neu5Gc) (lanes e) and 10 μg of human granulocyte gangliosides (lanes f) were used as references.

TLC immunostaining of G_{M1b} and $G_{D1\alpha}$ in the lungs, spleen, and thymus of control and TNFRp55 knockout mice.—Terminally sialylated ganglio-series gangliosides G_{M1b} and $G_{D1\alpha}$ have been reported to be typical gangliosides of the mouse leukocytes [34,35]. In this study G_{M1b}-type gangliosides were detected in the brain, lungs, spleen, and thymus of both TNFRp55 − / − and TNFRp55 + / − animals, but not in the liver and muscle. G_{M1b} and $G_{D1\alpha}$ are detectable on HPTLC plates with an anti-$GgOse_4Cer$ antibody after *V. cholerae* neuraminidase treatment, as demonstrated in two of our previous publications [36,37]. Murine lymphoma YAC-1 and lymphoreticular MDAY-D2 cell lines are known to express high levels of G_{M1b}-type gangliosides [38–40]. Ganglioside fractions from both cell lines were used as references and their major gangliosides are listed in Table 3. MDAY-D2 cells express Neu5Ac-substituted and lack Neu5Gc-containing gangliosides [40], whereas YAC-1 cells are characterized by high expression of Neu5Gc-substituted G_{M1b}-type gangliosides [39,41]. TLC overlay analysis of G_{M1b} and $G_{D1\alpha}$ in the lungs, spleen, and thymus of the TNFRp55 − / − strain is shown in Fig. 5(B) (lanes a, b, and c, respectively) in comparison to YAC-1 and MDAY-D2 cell lines (Fig. 5(B), lanes d and e, respectively), together with the corresponding resorcinol stain (Fig. 5(A)). G_{M1b} was not present in the lungs (Fig. 5(B), lane a) and only trace quantities were detected in the spleen and thymus of TNFRp55 − / − mice (Fig. 5(B), lanes b and c, respectively), separating at positions I (= G_{M1b}(Neu5Ac) with C_{24}-fatty acid) and II (= G_{M1b}(Neu5Ac) with C_{16}-fatty acid) of YAC-1 and MDAY-D2 reference gangliosides (see Table 3). In contrast, both G_{M1b}-species were abundant in the lungs, spleen, and thymus of control TNFRp55 + / − animals (Fig. 5(C), lanes a, b, and c, respectively). Two additional bands appeared in the ganglioside fraction of the thymus that chromatographed on the level of gangliosides VII (= $G_{D1\alpha}$(Neu5Ac, Neu5Ac) with C_{24}-fatty acid) and VIII (= $G_{D1\alpha}$(Neu5Ac, Neu5Ac) with C_{16}-fatty acid) of reference MDAY-D2 gangliosides. Both types of mice showed equal amounts of a G_{M1b}-positive band in the brain (data not shown), known to be a minor constituent in the mammalian brain [36,42]. These results clearly indicate the strong downregulation of terminally sialylated G_{M1b} ganglioside in the lungs, spleen, and thymus, and of $G_{D1\alpha}$ in the thymus of TNFRp55 − / − mice.

TLC immunostaining of GalNAc-G_{M1b} in lungs, spleen, and thymus of control and TNFRp55 knockout mice.—The ganglioside GalNAc-G_{M1b} has been reported to be a marker of mature and/or stimulated T lymphocytes [37,43]. The high specificity of the anti-GalNAc-G_{M1b} antibody that does not bind to any other ganglio- or neolacto-series gangliosides has been described in two reports [39,40]. It should be mentioned that this antibody does not discriminate between Neu5Ac- and Neu5Gc-substituted GalNAc-G_{M1b}, i.e., it also binds to GalNAc-G_{M1b}(Neu5Ac) and GalNAc-G_{M1b}(Neu5Gc). In the TLC overlay assay of ganglioside extracts from the lungs,

spleen, and thymus of TNFRp55 −/− mice this antibody stained only a trace band of GalNAc-G_{M1b} in the spleen fraction (Fig. 6(A), lane b), whereas in the control TNFRp55 +/− mice a strong band was present in the spleen fraction (Fig. 6(B), lane b) at position III (= GalNAc-G_{M1b}(Neu5Ac) with C_{16}-fatty acid and/or GalNAc-G_{M1b}(Neu5Gc) with C_{24}-fatty acid) of reference YAC-1 and MDAY-D2 gangliosides (see Table 3). Two positive GalNAc-G_{M1b} bands were detected in the lungs of the control TNFRp55 +/− mice at positions II and III (Fig. 6(B), lane a), most likely GalNAc-G_{M1b}(Neu5Ac) with C_{24}- and C_{16}-fatty acid, respectively, which were lacking in the lungs of TNFRp55 −/− mice (Fig. 6(A), lane a). The brain, liver, and muscle of both types of mice failed to express GalNAc-G_{M1b} (data not shown). Thus, GalNAc-G_{M1b} expression is downregulated in the lungs and spleen of TNFRp55 −/− mice.

Detection of neolacto-series gangliosides in tissues of control and TNFRp55 knockout mice.—Selective detection of terminally (α2-3)-sialylated neolacto-series gangliosides (IV^3nLc4, VI^3nLc6) involves immunostaining of TLC-separated gangliosides with anti-nLc4 antibody after *V. cholerae* neuraminidase treatment, whereas the visualization of IV^6nLc4 is feasible without enzyme treatment [44,45]. The presence of lactosamine-containing gangliosides in the brain, liver, lung, muscle, and spleen of both groups of mice was demonstrated using this method. TLC immunostaining with the anti-nLc4 antibody after neuraminidase treatment is shown in Fig. 7 for TNFRp55 −/− (Fig. 7(A), lanes a–e) and TNFRp55 +/− animals (Fig. 7(B), lanes a–e) in comparison to reference neolacto-series gangliosides from human granulocytes (Fig. 7(B), lane f). The most prominent difference between the two groups, in the brain extracts, was a strong expression of an (α2-3)-sialylated neolacto-core ganglioside (most likely VI^3nLc6) in TNFRp55 −/− mice (Fig. 7(A), lane a, arrow-head) compared with an extremely minor ganglioside in TNFRp55 +/− mice (Fig. 7(B), lane a, arrow-head). This terminally (α2-3)-sialylated ganglioside became apparent after neuraminidase treatment. The other strongly positive band above the arrow marks (Fig. 7(A) and (B), lanes a) was detectable with the anti-nLc4 antibody also without previous neuraminidase treatment in the brains of both strains (data not shown), thus representing an α2-6-sialylated neolacto-series ganglioside (most probably IV^6nLc4). The lungs of both groups of mice were characterized by high levels of neolacto-series gangliosides, chromatographing at positions of reference IV^3nLc4 and IV^6nLc4 of human granulocytes (Fig. 7(A) and (B), lanes c). A GSL band in the lungs of TNFRp55 −/−

Table 3
Major gangliosides from murine lymphoma YAC-1 and lymphoreticular MDAY-D2 cells

Ganglioside fraction	Fatty acid	Symbol [a]	Sialic acid	YAC-1	MDAY-D2
−II	24:0, 24:1	G_{M2}	Neu5Ac	−	+
−I	16:0	G_{M2}	Neu5Ac	−	+
0	24:0, 24:1	G_{M1a}	Neu5Ac	−	+
I	16:0	G_{M1a}	Neu5Ac	−	+
	24:0, 24:1	*G_{M1b}	Neu5Ac	+	+
II	16:0	*G_{M1b}	Neu5Ac	+	+
	24:0, 24:1	GalNAc-G_{M1b}	Neu5Ac	+	+
	24:0, 24:1	*G_{M1b}	Neu5Gc	+	−
III	16:0	*G_{M1b}	Neu5Gc	+	−
	16:0	GalNAc-G_{M1b}	Neu5Ac	+	+
	24:0, 24:1	GalNAc-G_{M1b}	Neu5Gc	+	−
IV	16:0	GalNAc-G_{M1b}	Neu5Gc	+	−
V	24:0, 24:1	G_{D1a}	Neu5Ac	−	+
VI	16:0	G_{D1a}	Neu5Ac	−	+
VII	24:0, 24:1	*$G_{D1\alpha}$	Neu5Ac	−	+
VIII	16:0	*$G_{D1\alpha}$	Neu5Ac	−	+

[a] G_{M1b} and $G_{D1\alpha}$ gangliosides detectable by immunostaining with anti-$GgOse_4Cer$ antibody after *V. cholerae* neuraminidase treatment are marked with asterisks; structural data drawn from Müthing et al. [39,40].

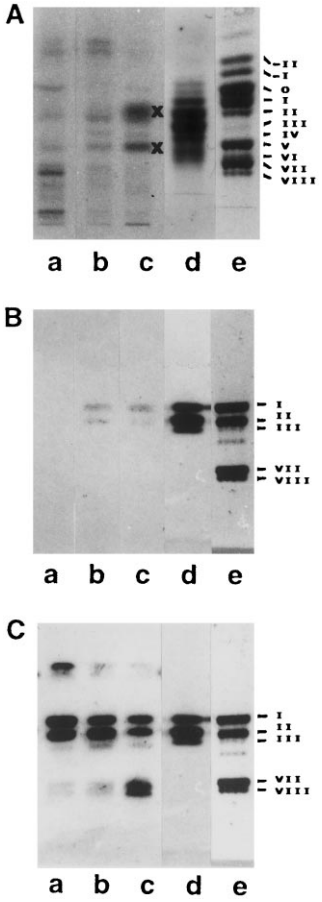

Fig. 5. Resorcinol stain (A) and TLC immunostaining of G_{M1b}-type gangliosides from the lungs, spleen, and thymus of TNFRp55 − / − (B) and TNFRp55 + / − mice (C). In panel A, ganglioside amounts corresponding to 60 mg (lung, lane a) and 40 mg wet weight (spleen and thymus, lanes b and c, respectively) were chromatographed together with 10 μg YAC-1 (lane d) and 10 μg MDAY-D2 gangliosides (lane e). In panels B and C, one third of ganglioside quantities were applied in the same order. YAC-1 and MDAY-D2 gangliosides are marked with roman numerals from (− II) to VIII and their structures are given in Table 3. Crosses indicate resorcinol negative bands.

mice (Fig. 7(A), lane c, arrow-head), separating at the position VI^3nLc6 of human granulocytes (Fig. 7(B), lane f), was considerably reduced in the lungs of TNFRp + / − mice (Fig. 7(B), lane c). The same was found for the muscle (Fig. 7(A) and (B), lanes d), where this (α2-3)-sialylated neolacto-core ganglioside (most likely VI^3nLc6) represented the major neolacto-type ganglioside in the muscle of TNFRp55 − / − animals (Fig. 7(A), lane d). Spleens of both groups showed low (Fig. 7, lanes e) and the liver only trace quantities of lacto type 2 gangliosides (Fig. 7, lanes b), whereas the ganglioside extract of the thymus did not react with this antibody (data not shown). As a general feature, the brain and lungs of TNFRp55 − / − animals were characterized by an enhanced expression of an (α2-3)-sialylated ganglioside, most likely VI^3nLc6, whereas control TNFRp55 + / − mice failed to produce relevant amounts of this GSL.

Detection of G_{M1a}-type gangliosides in tissues of control and TNFRp55 knockout mice.—The expression patterns of G_{M1a}-type gangliosides in tissues of mice homo- or heterozygous for the TNFRp55 gene knockout were very similar. The extracts from the lungs, spleen, and thymus showed triple band patterns (most clearly for G_{M1a}), which did not occur in the brain, liver, or muscle fractions. These triple bands are typical for murine lymphocytes [46,47] due to substitution with Neu5Ac/

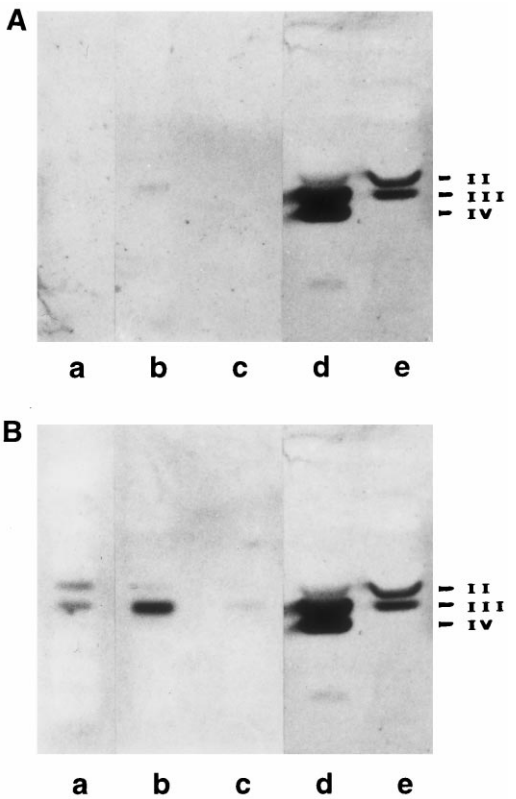

Fig. 6. Anti-GalNAc-G_{M1b} TLC immunostaining of ganglioside fractions from the lungs, spleen, and thymus of TNFRp55 − / − (A) and control TNFRp55 + / − mice (B). In both panels ganglioside amounts corresponding to 20 mg lung (lanes a) and 13.3 mg spleen and thymus wet weight (lanes b and c, respectively) were chromatographed together with 3 μg YAC-1 (lanes d) and 10 μg MDAY-D2 gangliosides (lanes e). YAC-1 and MDAY-D2 gangliosides are marked with roman numerals according to Table 3.

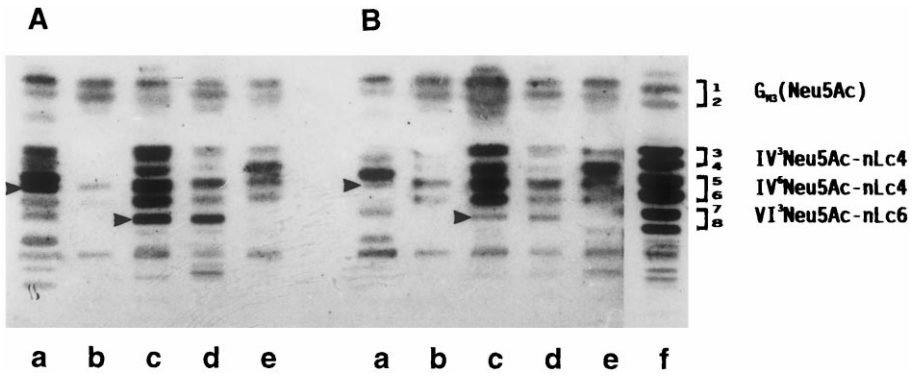

Fig. 7. Detection of neolacto-series gangliosides in the brain, liver, lungs, muscle, and spleen of TNFRp55 −/− (A) and control TNFRp55 +/− mice (B). In both panels ganglioside amounts corresponding to 3.3 mg brain (lanes a), 13.3 mg liver (lanes b), 20 mg lung and muscle (lanes c and d, respectively), and 13.3 mg spleen wet weight (lanes e) were chromatographed together with 2.5 μg human granulocyte gangliosides (lane f). The TLC immunostain was performed with anti-nLcOse$_4$Cer antibody after *V. cholerae* neuraminidase treatment.

Neu5Gc and C_{24}-/C_{16}-fatty acids (data not shown).

3. Discussion

Among all mouse organs and tissues, the brain is characterized by gangliosides substituted exclusively with Neu5Ac; all other organs and tissues contain considerable amounts of Neu5Gc, particularly the liver, where Neu5Gc represents the major lipid-bound sialic acid. It is unlikely that Neu5Gc has one specific function but it may modulate the functions exerted by sialic acids [19]. Concerning the role of CMP-Neu5Ac hydroxylase in regulating the incorporation of Neu5Gc into glycoconjugates, the relative levels of Neu5Gc and Neu5Ac in the rat and mouse liver [48], as well as in several related mouse lymphoma cell lines, correlated with the activity of CMP-Neu5Ac hydroxylase [49]. Using rat small-intestine mucosal cells, Bouhours and Bouhours [50] showed that the increase in the G_{M3}(Neu5Gc) content correlated with the increase in the activity of CMP-Neu5Ac hydroxylase activity. From this data we can conclude that the differences in Neu5Gc expression in the tissues of TNFRp55 −/− and control TNFRp55 +/− mice should be due to altered hydroxylase activities in respective organs. Among the tissues and organs analyzed in this study, the muscle and brain of TNFRp55 −/− mice showed considerable increase in the total lipid-bound sialic acids compared with the control animals. Because whole tissues were analyzed, further studies are needed to determine cell-type-specific expression of gangliosides in these organs.

G_{M1b} was detected in the spleen and thymus and $G_{D1\alpha}$ in the thymus of the control TNFRp55 +/− mice. These structures were almost undetectable in TNFRp55 −/− animals, indicating strong downregulation of terminally sialylated gangliosides with a GgOse$_4$Cer backbone in the absence of TNFRp55 receptor. G_{M1b} was also found in large quantity in the lungs of the control TNFRp55 +/− mice, whereas even trace amounts could not be detected in TNFRp55 −/− animals. Similarity between the G_{M1b} expression in the lungs and lymphoid organs is not surprising because G_{M1b} is known to be a typical ganglioside of murine T cells [34,37] and macrophages [35,51] and lungs harbour T cells and macrophages. Thus, G_{M1b} expression seems to be due to the presence of these cells in the murine lungs. GalNAc-G_{M1b}, the elongation product of G_{M1b}, was found in considerable quantities in the spleen and lungs and in moderate quantity in the thymus of TNFRp55 +/− mice. This correlates with previous findings by us and others that GalNAc-G_{M1b} is a marker of activated T cells and macrophages [37,43,51]. In a similar manner to G_{M1b}, GalNAc-G_{M1b} expression was drastically reduced in the lungs, spleen and thymus of the TNFRp55 −/− mice, indicating that the signaling via this receptor is indeed involved in

the acquisition of the ganglioside phenotype of lymphoid cells.

Up until now only a small amount of data concerning neolacto-type and related gangliosides in the mouse has been available. Large amounts of terminally sialylated $nLcOse_4Cer$ and $nLcOse_6Cer$ were detected in both TNFRp55 −/− and control TNFRp55 +/− mice, particularly in the brain and lungs, and to a lesser extent in the muscle and spleen. However, nothing is known at this time about the cell-type-specific expression of neolacto-series gangliosides in murine organs. Our data would indicate that signaling through the TNFRp55 receptor is involved in the expression of these gangliosides in the mouse.

The ability of gangliosides to modulate growth factor receptor signal transduction has been intensively studied. For example, the tyrosine kinase activity and its signal transduction is inhibited by G_{M3} [52,53]. G_{M3} also has immunomodulatory capacities, such as inhibition of the natural killer cell activity [54] and induction of CD4 internalization in human peripheral blood T lymphocytes [55]. Furthermore, G_{M3} and related gangliosides (G_{D3}, G_{D1a}, G_{M2}, and G_{M1}) can suppress TNF production in human monocytes [25]. The major difference in the ganglioside expression among the five tissues analyzed in our study was almost complete absence of G_{M3} in the lungs of TNFRp55 −/− compared with control TNFRp55 +/− mice. G_{M3} is abundant in the adult lungs and its appearance changes during the prenatal and postnatal development [56,57]. Its role in the lungs is unknown, but is probably not related to the interaction with pulmonary surfactant apoproteins [57]. The lungs of adult TNFRp55 −/− mice lack obvious morphological pathology (our unpublished data), but this does not exclude the possible role of signaling through this receptor in the lung homeostasis.

GSLs have been implicated in the immune cell circulation and/or localization of cells in lymphoid organs [15]. TNF can influence the activity of sialyltransferases in endothelial cells in vitro, which subsequently changes cell attachment and migration [58]. With this in mind, our in vivo data indicate that TNF-regulated expression of gangliosides during development may play a role in directing the homing and morphological compartmentalization of lymphoid organs, resulting in a typical phenotype of TNFRp55-deficient mice [2,4,5]. Considering the recent advances in understanding the biosynthesis of gangliosides (reviewed by Lloyd and Furukawa [59]), an in vivo approach, such as the one used in our study, may be a suitable model for studying the role of gangliosides in cell functions, and gene-disruption approaches may demonstrate novel functions of gangliosides both in health and disease.

4. Experimental

Animals.—Mice lacking the gene for the tumor necrosis factor receptor p55 were originally generated by Pfeffer et al. [2]. They were bred onto C57BL/6 background and kept under standard housing conditions (laboratory rodent chow and water ad libitum and 12 h light–dark cycle) at the Animal Facility of the Rijeka University School of Medicine (Rijeka, Croatia). Mice used in the study were either homozygous (TNFRp55 −/−) or heterozygous (TNFRp55 +/−) for the TNFRp55 gene knockout. For the study, males aged 10 weeks were killed by cervical dislocation under CO_2 anesthesia, the tissues were dissected out and stored at −20 °C until GSL extraction.

Isolation of GSLs from tissues.—Brains, livers, lungs, thigh muscle, spleens, and thymi were dissected from 10 animals of each group. Identical tissues were pooled, minced with a scalpel, suspended in distilled water in a 1:2 ratio (w/v), homogenized for 10 min with a dispersing tool (Polytron PT1200C, Kinematica AG, Littau/Luzern, Switzerland), and isolated according to standard procedures [60]. Chloroform and MeOH of analytical grade (E. Merck, Darmstadt, Germany) were distilled before use. Briefly, GSLs were extracted with a 2:1 mixture of $CHCl_3$–MeOH, 1:1 $CHCl_3$–MeOH, and 1:2 $CHCl_3$–MeOH (10-fold volumes of the tissue wet weight) for 30 min with sonication. The combined extracts were evaporated, resuspended in a 30:60:8

mixture of $CHCl_3$–MeOH–water, and gangliosides were isolated by anion-exchange chromatography on DEAE-Sepharose CL-6B (Pharmacia Fine Chemicals, Freiburg, Germany) as reported previously [34]. The ganglioside fraction was incubated for 1 h at 37 °C in aq 1 N NaOH to saponify phospholipids, followed by neutralization with HOAc and dialysis. Gangliosides were further purified by adsorption chromatography on Iatrobeads 6RS-8060 (Macherey-Nagel, Düren, Germany) as described by Ueno et al. [61].

After column chromatography purifications, final ganglioside fractions were adjusted to defined volumes of 2:1 $CHCl_3$–MeOH corresponding to 4 mg wet weight per μL for the liver and 2 mg wet weight per μL for all other tissues.

Thin-layer chromatography and reference gangliosides.—Gangliosides were separated on Silica Gel 60 precoated high-performance thin-layer chromatography plates (HPTLC-plates, size 10 × 10 cm, thickness 0.2 mm, E. Merck; Art. No. 5633) using a 120:85:20 mixture of $CHCl_3$–MeOH–water (each by vol.) with 2 mM $CaCl_2$, and visualized with resorcinol [62].

A ganglioside mixture composed of G_{M3}(Neu5Ac), IV^3Neu5Ac-nLcOse$_4$Cer (IV^3nLc4), IV^6Neu5Ac-nLcOse$_4$Cer (IV^6nLc4), and VI^3Neu5Ac-nLcOse$_6$Cer (VI^3nLc6) was isolated from human granulocytes as previously described [30,63]. G_{M3}(Neu5Gc) was purified from a mouse–mouse hybridoma [32].

Gangliosides from murine T lymphoma YAC-1 and lymphoreticular tumor cell line MDAY-D2 were isolated according to established procedures [39,40] (see Table 3). Human brain gangliosides were purchased from Supelco Inc. (Bellefonte, PA, USA).

Determination of sialic acids.—Neu5Ac and Neu5Gc of gangliosides were identified as their fluorescent derivatives by HPLC essentially as described by Hara et al. [64]. Sialic acids were released from gangliosides with 25 mM H_2SO_4 (80 °C, 90 min) and converted with 1,2-diamino-4,5-methylenedioxybenzene (DMB; Sigma, Deisenhofen, Germany) into fluorescent derivatives. Sialic acids were separated by isocratic elution with 9:7:110 MeCN–MeOH–water (by vol.) on an RP_{18} column (4.6 × 125 mm Supersphere, 4 μm particle size, Bischoff Chromatography, Leonberg, Germany) with a flow rate of 1.2 mL/min. Reference Neu5Ac was from Biomol (Hamburg, Germany; Cat. No. 01103) and Neu5Gc from Sigma (Cat. No. G-2755).

Antibodies and cholera toxin B subunit (choleragenoid).—Polyclonal chicken anti-G_{M3}(Neu5Ac) and anti-G_{M3}(Neu5Gc) antibodies have been characterized in our previous reports [31,32]. Rabbit anti-GgOse$_4$Cer antiserum used for the detection of G_{M1b} and $G_{D1\alpha}$ has been described in earlier publications [36,37]. Highly specific chicken anti-GalNAc-G_{M1b} antibody has been described in detail elsewhere [39,40]. Chicken anti-nLcOse$_4$Cer antibody used for the analysis of neolacto-series gangliosides has been characterized in our earlier publications [31,44,65]. Cholera toxin B subunit (= choleragenoid) specific for ganglioside G_{M1} was from Sigma (No. C-7771) and goat anti-choleragenoid antiserum from Calbiochem (Frankfurt a.M., Germany; No. 227040).

TLC immunostaining.—Overlay technique was carried out according to Magnani et al. [66] with some modifications, which have been described in two recent reviews concerning the details of the TLC immunostaining procedure [29,67]. All GSL-specific antibodies were used at 1:1000 dilutions. Secondary rabbit anti-chicken IgG, goat anti-rabbit IgG, and rabbit anti-goat IgG antisera, all affinity chromatography-purified and labeled with alkaline phosphatase (0.6 mg/mL), were purchased from Dianova and used as 1:2000 dilutions (see below). Briefly, the silica gel was fixed with polyisobutylmethacrylate and unspecific protein binding was blocked by a 15 min incubation of the plate with solution A (PBS supplemented with 1% bovine serum albumin and 0.02% NaN_3). The plates were then overlayed for 1 h with anti-GSL antibodies and unbound antibodies were removed by washing each plate five times with solution B (0.05% Tween 21, 0.02% NaN_3 in PBS). After 1 h incubation with secondary antibodies, diluted 1:2000 in solution A (see above), the plates were washed again followed by two-fold rins-

ing with glycine buffer (0.1 M glycine, 1 mM $ZnCl_2$, 1 mM $MgCl_2$, pH 10.4), to remove phosphate. Bound antibodies were visualized with 0.05% (w/v) 5-bromo-4-chloro-3-indolylphosphate (Biomol, Hamburg, Germany) in glycine buffer.

TLC immunostaining of G_{M1b}-type gangliosides.—Terminally sialylated gangliosides with $GgOse_4Cer$ backbone (G_{M1b}, $G_{D1\alpha}$) were detected as described previously [36]. After chromatography of gangliosides and silica gel fixation, the plate was incubated for 2 h at 37 °C with 2.5 mU/mL *V. cholerae* neuraminidase (Behring Werke AG, Marburg, Germany) in 0.05 M sodium acetate, 9 mM $CaCl_2$, pH 5.5. Desialylated gangliosides were immunostained with polyclonal anti-$GgOse_4Cer$ antibody (see above).

TLC immunostaining of neolacto-series gangliosides.—Neuraminidase treatment of neolacto-series gangliosides with (α2-3)-substituted sialic acid is necessary prior to immunostaining with anti-$nLcOse_4Cer$ antibody, whereas (α2-6)-sialylated neolacto-type gangliosides can be detected without enzyme treatment since sialylation at the position 6 of the terminal galactose does not hinder recognition. Fixed silica gel plates were incubated with 2.5 mU/mL *V. cholerae* neuraminidase (Behring Werke AG) for 2 h at 37 °C in the buffer described above, followed by immunostaining with anti-$nLcOse_4Cer$ antibody (for details see [31,44]). Neolacto-series gangliosides from human granulocytes, composed of G_{M3}(Neu5Ac), IV^3nLc4, IV^6nLc4, and VI^3nLc6 served as references [63].

TLC detection of G_{M1a}-type gangliosides.—The TLC binding assay using choleragenoid for specific detection of G_{M1} was developed by Magnani et al. [68] and was used according to the modifications described in previous publications [46,69]. A fixed silica gel plate was overlayed with 250 ng/mL choleragenoid (Sigma) diluted in solution A for 2 h at room temperature, followed by goat anti-choleragenoid (Calbiochem) and secondary rabbit anti-goat IgG antibody incubation (both diluted 1:2000). Bound antibodies were visualized as described above. To reveal the presence of G_{D1a}, G_{D1b}, and G_{T1b}, the plates were incubated with 5 mU/mL *V. cholerae* neuraminidase (2 h, 37 °C) in the buffer described above, prior to combined choleragenoid immunostaining. This technique was originally developed by Wu and Ledeen [70].

Acknowledgements

This work was financially supported by the Deutsche Forschungsgemeinschaft (DFG), Sonderforschungsbereich 549 (Project B07). We thank Professor Dr Klaus Pfeffer (Technical University of Munich, Germany) for his kind gift of TNFR1 knockout mice.

References

[1] R.J. Armitage, *Curr. Opin. Immunol.*, 6 (1994) 407–413.
[2] K. Pfeffer, T. Matsuyama, T.M. Kündig, A. Wakeham, K. Kishihara, A. Shahinian, K. Wiegmann, P.S. Ohashi, M. Krönke, T.W. Mak, *Cell*, 73 (1993) 457–467.
[3] J. Rothe, W. Lesslauer, H. Lötscher, Y. Lang, P. Koebel, F. Köntgen, A. Althage, R. Zinkernagel, M. Steinmetz, H. Bluethmann, *Nature*, 364 (1993) 798–802.
[4] M. Le Hir, H. Bluethmann, M.H. Kosco-Vilbois, M. Müller, F. di Padova, M. Moore, B. Ryffel, H.P. Eugster, *J. Exp. Med.*, 183 (1996) 2367–2372.
[5] B. Neumann, A. Luz, K. Pfeffer, B. Holzmann, *J. Exp. Med.*, 184 (1996) 259–264.
[6] S.L. Erickson, F.J. de Sauvage, K. Kikly, K. Carver-Moore, S. Pitts-Meek, N. Gillett, K.C.F. Sheehan, R.D. Schreiber, D.V. Goeddel, M.W. Moore, *Nature*, 372 (1994) 560–563.
[7] J.J. Peschon, D.S. Torrance, K.L. Stocking, M.B. Glaccum, C. Otten, C.R. Willis, K. Charrier, P.J. Morrissey, C.B. Ware, K.M. Mohler, *J. Immunol.*, 160 (1998) 943–952.
[8] K. Wiegmann, S. Schütze, E. Kampen, A. Himmler, T. Machleidt, M. Krönke, *J. Biol. Chem.*, 267 (1992) 17997–18001.
[9] S. Schütze, K. Potthoff, T. Machleidt, D. Berkovic, K. Wiegmann, M. Krönke, *Cell*, 71 (1992) 765–776.
[10] Y.A. Hannun, *J. Biol. Chem.*, 269 (1994) 3125–3128.
[11] S. Mathias, K.A. Dressler, R.N. Kolesnick, *Proc. Natl. Acad. Sci. USA*, 88 (1991) 10009–10013.
[12] G. van Echten, K. Sandhoff, *J. Biol. Chem.*, 268 (1993) 5341–5344.
[13] R.L. Schnaar, *Glycobiology*, 1 (1991) 477–485.
[14] P.R. Crocker, T. Feizi, *Curr. Opin. Struct. Biol.*, 6 (1996) 679–691.
[15] S.-I. Hakomori, Y. Igarashi, *J. Biochem.*, 118 (1995) 1091–1103.
[16] K. Simons, E. Ikonen, *Nature*, 387 (1997) 569–572.
[17] S.-I. Hakomori, K. Handa, K. Iwabuchi, S. Yamamura, A. Prinetti, *Glycobiology*, 8 (1998) xi–xix.
[18] A. Varki, *Glycobiology*, 2 (1992) 25–40.
[19] R. Schauer, S. Kelm, G. Reuter, P. Roggentin, L. Shaw, in A. Rosenberg (Ed.), *Biology of the Sialic Acids*, Plenum Press, New York, 1995, pp. 7–67.

[20] R. Li, N. Villacreses, S. Ladisch, *Cancer Res.*, 55 (1995) 211–214.
[21] H. Offner, T. Thieme, A.A. Vandenbark, *J. Immunol.*, 139 (1987) 3295–3305.
[22] H. Repke, E. Barber, S. Ulbricht, K. Buchner, F. Hucho, R. Kopp, H. Scholz, C.E. Rudd, W.A. Haseltine, *J. Immunol.*, 149 (1992) 2585–2591.
[23] L.D. Bergelson, *Immunol. Today*, 16 (1995) 483–486.
[24] A. Heitger, S. Ladisch, *Biochim. Biophys. Acta*, 1303 (1996) 161–168.
[25] H.W.L. Ziegler-Heitbrock, E. Käfferlein, J.G. Haas, N. Meyer, M. Ströbel, C. Weber, D. Flieger, *J. Immunol.*, 148 (1992) 1753–1758.
[26] T. Koike, K. Fehsel, J. Zielasek, H. Kolb, V. Burkart, *Immunol. Lett.*, 35 (1993) 207–212.
[27] M.L. Neale, K.M. Taylor, N. Matthews, *Cytokine*, 3 (1991) 250–256.
[28] K. Furukawa, Y. Arita, N. Satomi, M. Eisinger, K.O. Lloyd, *Arch. Biochem. Biophys.*, 281 (1990) 70–75.
[29] J. Müthing, *J. Chromatogr. A*, 720 (1996) 3–25.
[30] J. Müthing, R. Spanbroek, J. Peter-Katalinić, F.-G. Hanisch, C. Hanski, A. Hasegawa, F. Unland, J. Lehmann, H. Tschesche, H. Egge, *Glycobiology*, 6 (1996) 147–156.
[31] J. Müthing, U. Maurer, K. Sostarić, U. Neumann, H. Brandt, S. Duvar, J. Peter-Katalinić, S. Weber-Schürholz, *J. Biochem.*, 115 (1994) 248–256.
[32] J. Müthing, H. Steuer, J. Peter-Katalinić, U. Marx, U. Bethke, U. Neumann, J. Lehmann, *J. Biochem.*, 116 (1994) 64–73.
[33] S. Duvar, J. Peter-Katalinić, F.-G. Hanisch, J. Müthing, *Glycobiology*, 7 (1997) 1099–1109.
[34] J. Müthing, H. Egge, B. Kniep, P.F. Mühlradt, *Eur. J. Biochem.*, 163 (1987) 407–416.
[35] H.C. Yohe, C.L. Cuny, L.J. Macala, M. Saito, W.J. McMurray, J.L. Ryan, *J. Immunol.*, 146 (1991) 1900–1908.
[36] J. Müthing, P.F. Mühlradt, *Anal. Biochem.*, 173 (1988) 10–17.
[37] J. Müthing, B. Schwinzer, J. Peter-Katalinić, H. Egge, P.F. Mühlradt, *Biochemistry*, 28 (1989) 2923–2929.
[38] S. Laferté, M.M. Fukuda, M. Fukuda, A. Dell, J.W. Dennis, *Cancer Res.*, 47 (1987) 150–159.
[39] J. Müthing, J. Peter-Katalinić, F.-G. Hanisch, U. Neumann, *Glycoconjugate J.*, 8 (1991) 414–423.
[40] J. Müthing, J. Peter-Katalinić, F.-G. Hanisch, F. Unland, J. Lehmann, *Glycoconjugate J.*, 11 (1994) 153–162.
[41] R. Li, D. Gage, S. Ladisch, *Biochim. Biophys. Acta*, 1170 (1993) 283–290.
[42] T. Ariga, R.K. Yu, *J. Lipid Res.*, 28 (1987) 285–291.
[43] K. Horikawa, M. Yamasaki, M. Iwamori, H. Nakakuma, K. Takatsuki, Y. Nagai, *Glycoconjugate J.*, 8 (1991) 354–360.
[44] J. Müthing, U. Neumann, *Biomed. Chromatogr.*, 7 (1993) 158–161.
[45] J. Müthing, S. Duvar, D. Heitmann, F.-G. Hanisch, U. Neumann, G. Lochnit, R. Geyer, J. Peter-Katalinić, *Glycobiology*, 9 (1999) 459–468.
[46] A. Pörtner, J. Peter-Katalinić, H. Brade, F. Unland, H. Büntemeyer, J. Müthing, *Biochemistry*, 32 (1993) 12685–12693.
[47] J. Müthing, *Glycoconjugate J.*, 14 (1997) 241–248.
[48] A. Lepers, L. Shaw, P. Schneckenburger, R. Cacan, A. Verbert, R. Schauer, *Eur. J. Biochem.*, 193 (1990) 715–723.
[49] L. Shaw, S. Yousefi, J.W. Dennis, R. Schauer, *Glycoconjugate J.*, 8 (1991) 434–441.
[50] J.-F. Bouhours, D. Bouhours, *J. Biol. Chem.*, 264 (1989) 16992–16999.
[51] L.J. Macala, H.C. Yohe, *Glycobiology*, 5 (1995) 67–75.
[52] E.G. Bremer, J. Schlessinger, S.-I. Hakomori, *J. Biol. Chem.*, 261 (1986) 2434–2440.
[53] A. Rebbaa, J. Hurh, H. Yamamoto, D.S. Kersey, E.G. Bremer, *Glycobiology*, 6 (1996) 399–406.
[54] L.D. Bergelson, E.V. Dyatlovitskaya, T.E. Klynchareva, E.V. Kryukova, A.F. Lemenovskaya, V.A. Matveeva, E.V. Sinitsyna, *Eur. J. Immunol.*, 19 (1989) 1979–1983.
[55] M. Sorice, A. Pavan, R. Misasi, T. Sansolini, T. Garofalo, L. Lenti, G.M. Pontieri, L. Frati, M.R. Torrisi, *Scand. J. Immunol.*, 41 (1995) 148–156.
[56] T.N. Seyfried, *Dev. Biol.*, 123 (1987) 286–291.
[57] K. Momoeda, K. Hirota, T. Utsuki, Y. Tsuchida, K. Hanaoka, M. Iwamori, *J. Biochem.*, 119 (1996) 1189–1195.
[58] K. Hanasaki, A. Varki, I. Stamenkovic, M.P. Bevilacqua, *J. Biol. Chem.*, 269 (1994) 10637–10643.
[59] K.O. Lloyd, K. Furukawa, *Glycoconjugate J.*, 15 (1998) 627–636.
[60] R.W. Ledeen, R.K. Yu, *Methods Enzymol.*, 83 (1982) 139–191.
[61] K. Ueno, S. Ando, R.K. Yu, *J. Lipid Res.*, 19 (1978) 863–871.
[62] L. Svennerholm, *Biochim. Biophys. Acta*, 24 (1957) 604–611.
[63] J. Müthing, F. Unland, D. Heitmann, M. Orlich, F.-G. Hanisch, J. Peter-Katalinić, V. Knäuper, H. Tschesche, S. Kelm, R. Schauer, J. Lehmann, *Glycoconjugate J.*, 10 (1993) 120–126.
[64] S. Hara, Y. Takemori, M. Yamaguchi, M. Nakamura, Y. Ohkura, *Anal. Biochem.*, 164 (1987) 138–145.
[65] J. Müthing, S.E. Kemminer, *Anal. Biochem.*, 238 (1996) 195–202.
[66] J.L. Magnani, B. Nilsson, M. Brockhaus, D. Zopf, Z. Steplewski, H. Koprowski, V. Ginsburg, *J. Biol. Chem.*, 257 (1982) 14365–14369.
[67] J. Müthing, in E.F. Hounsell (Ed.), *Methods in Molecular Biology*, Vol. 76: *Glycoanalysis Protocols*, Humana Press, Totowa, NJ, 1998, pp. 183–195.
[68] J.L. Magnani, D.F. Smith, V. Ginsburg, *Anal. Biochem.*, 109 (1980) 399–402.
[69] J. Müthing, A. Pörtner, V. Jäger, *Glycoconjugate J.*, 9 (1992) 265–273.
[70] G. Wu, R. Ledeen, *Anal. Biochem.*, 171 (1988) 368–375.
[71] IUPAC–IUB Commission on biochemical nomenclature, *Eur. J. Biochem.*, 79 (1977) 11–21.
[72] L. Svennerholm, *J. Neurochem.*, 10 (1963) 613–623.